

INFLUENCE OF TRANSIENT NEAR-TIP STRESS FIELD ON HYDROGEN ASSISTED CRACKING

J. Toribio and V. Kharin\*

The effects of fatigue pre-cracking and loading rate on hydrogen assisted fracture were studied to elucidate the influence of the corresponding stress-pattern on hydrogen diffusion towards rupture sites in the crack tip zone. A finite element procedure was used to model cyclic loading using an elastoplastic large-deformation analysis followed by stress-assisted diffusion. In the sustained load case the test duration for reliable evaluation of the hydrogen assisted cracking threshold was estimated. For rising load conditions, fatigue crack closure (residual) stresses due to pre-cracking affect near-tip hydrogen diffusion and consequently the initiation of hydrogen assisted fracture.

INTRODUCTION

Hydrogen can promote metals fracture (Nelson (1)) and the process of hydrogen assisted cracking (HAC) is limited by hydrogen supply to rupture sites. Hydrogen diffusion in metal has been proposed as the key transport mode controlling the kinetics of HAC (van Leeuwen (2)). Modelling of hydrogen entry in the crack tip region has received much attention as a part of the HAC theory (Toribio and Kharin (3)). However, several items still require elucidation, among them the effects of the pre-HAC crack history (i.e., fatigue pre-cracking) and of loading dynamics during hydrogenation. Study of their interaction is of particular worth to rationalise the accelerated evaluation of materials susceptibility to HAC using dynamic rising loading, e.g., the slow strain rate testing (SSRT) technique.

Within the framework of the diffusion theory of HAC (2,3), the problem of hydrogen diffusion affected by the crack-tip stress field is treated in this paper coupled with explicit high-resolution finite-deformation analysis of the cracked elastoplastic solid. Numerical simulation of SSRT situation is performed following the variation of the stress field from the compressive residual stresses at removed load state after fatigue cycling to the tensile stress distribution at elevated load.

---

\* Department of Materials Science, University of La Coruña, E.T.S.I. Caminos, Campus de Elviña, 15071 La Coruña, Spain.

DESCRIPTION OF THE MODEL

HAC is governed by a critical combination of hydrogen concentration  $C$  and stress-strain state in a material cell, i.e., a critical value of concentration  $C_{cr}$  exists as a function of stress and strain tensors,  $\sigma$  and  $\epsilon$  respectively. Crack advance occurs when concentration of hydrogen accumulated with time  $t$  reaches  $C_{cr}$  in a relevant location  $x_c$  near the crack tip (3):

$$C(x_c, t) = C_{cr}(\sigma(x_c, t), \epsilon(x_c, t)) \quad (1)$$

The left-hand part in (1) is defined by hydrogen transport and the right-hand one depends on attained load level. Under certain conditions, hydrogen diffusion in metal is the rate-controlling mechanism of hydrogen supply to the fracture process zone (3). The equation of stress-strain assisted diffusion is (cf. (3)):

$$\frac{dC}{dt} = -\nabla \cdot \left[ D \nabla C - DC \left( \frac{V_H}{RT} \nabla \sigma + \frac{\nabla K_{s0}(\epsilon_{eq}^p)}{K_{s0}(\epsilon_{eq}^p)} \right) \right] \quad (2)$$

where  $D$  is the diffusion coefficient,  $V_H$  the partial molar volume of hydrogen,  $R$  the universal gas constant,  $T$  the absolute temperature,  $\sigma$  the hydrostatic stress,  $\epsilon_{eq}^p$  the equivalent plastic strain and  $K_{s0}$  the strain-only dependent component of the hydrogen solubility coefficient.

Large deformations are essential for near-tip diffusion since they notably affect the stress-strain state and change diffusion distances in the zone of interest. To solve the mechanical portion of the problem of stress-assisted diffusion at large deformations, the nonlinear finite element code MARC (4) was employed and complemented with a diffusion-related module. The standard weighted residual process was used to build-up a finite-element approximation of the initial-boundary value problem (2) in material coordinates taking as reference the instantaneous deformed configuration of the solid, and Galerkin scheme was applied for time-domain integration of the finite element equations system. The study is confined to small-scale yielding in fracture mechanics sense, so the tensors  $\sigma$  and  $\epsilon$  in the crack tip zone are dominated by the stress intensity factor  $K$ . This allows a quite general analysis in terms of  $K(t) \propto \sigma_{app}(t)$  not limited to a particular body geometry and loading.

To simulate stress-assisted diffusion, a 2D model of the double-edge-cracked panel in tension is adopted. Initial crack tip width  $b_0$  and mechanical constants are kept the same as in the previous mechanical study (Toribio and Kharin (5)):  $b_0 = 5 \mu\text{m}$ , Young modulus  $E = 200 \text{ GPa}$ , Poisson ratio  $\mu = 0.3$ , tensile yield stress  $\sigma_Y = 600 \text{ MPa}$ . Hydrogen-related characteristics are (2)  $D = 10^{-13} \text{ m}^2/\text{s}$ ,  $V_H = 2 \text{ cm}^3/\text{mol}$ . Diffusion in a stationary stress field under sustained load was performed first to reveal some items related to the HAC threshold  $K_{th}$ . A reference value of  $K$  was taken  $K_R = 60 \text{ MPam}^{1/2}$  which may be a candidate for the threshold  $K_{th}$  (Mayville et al. (6)). In the next phase, diffusion in transient stress field under SSRT conditions was considered with constant stress intensity rate  $dK/dt = K^\bullet$  applied after pre-cracking by fatigue between zero and  $K_{max}$  (Fig. 1a, insert).  $K_R = 60 \text{ MPam}^{1/2}$  was used as a "candidate threshold", and  $K_{max} = 0.5K_R$  as the advised pre-cracking

limit (Judy et al. (7)). The range of  $K^{\bullet}$  between 0.015 and 15 MPam<sup>1/2</sup>/min corresponding to common experimental practice (6) was covered.

The key items for HAC are the near-tip distributions of  $\sigma$  and  $\varepsilon_{eq}^p$  represented in Fig. 1 as functions of the distance from the material point to the crack tip in the undeformed configuration  $X$  divided by the current crack tip opening displacement  $\delta_t$ . The positive stress gradient associated with tension favours hydrogen flux into metal, and the negative one at compression causes a retardation effect. The contribution of these compressive stresses is expected to be important for the near-tip diffusion, and consequently for the initiation of HAC.

## RESULTS AND DISCUSSION

As a first approach, hydrogen diffusion was modelled in a 1D approximation, i.e., on the  $x$ -axis along the crack line where element discretization, stresses and strains corresponded to the 2D mechanical solution (elastoplastic finite element analysis).

### Sustained Load Case

Fig. 2 displays the calculated hydrogen concentration along the crack line under sustained load together with the closed form asymptotic solution by Kharin and Toribio (8). Fig. 3 presents the variation of concentration in the material points of interest with regard to HAC: the point  $x_{m\sigma} \approx 2.3\delta_t$  where the maximum tensile stresses are attained and the point  $x_{m\varepsilon} \approx \delta_t$  which marks the zone of steeply increasing plastic strain (Fig. 1a). These may be fracture places  $x_c$  depending on the operative fracture mechanism (stress- or strain-controlled).

These data are related to  $K_{th}$  testing in which a series of sustained  $K$ -values is tried if crack does not start to grow within a certain time  $t_B$  (Turnbull (9));  $t_B$  must be about the diffusion time  $t_{ss}$  to attain at  $x_c$  the the upper bound concentration level fixed by the steady-state value,  $C(x_c, t_{ss}) \approx C_{eq}(x_c)$ , the latter being able to satisfy the criterion (1). Hydrogen diffusion solution may serve to substantiate the testing time  $t_B \approx t_{ss}$  (8). Plots in Fig. 3a confirm that the simple asymptotic (8) and numerical solutions are fairly close at  $x_{m\sigma}$ , and the first one can be used to evaluate  $t_B$  at stress-controlled fracture mechanism estimating  $x_c \approx x_{m\sigma}$ . For possible strain-controlled fracture at  $x_c \approx x_{m\varepsilon}$  the asymptotic solution goes slower and underestimates  $t_B$  since the times of entry of both solutions into the narrow 5%-width tolerance band near the required  $C_{eq}$ -level differ substantially.

### Rising Load Case

When the SSRT technique is used for HAC testing (9), a dynamic test is performed with rising load to pass the whole stress intensity range up to detecting a crack growth initiation at some  $K_R$  which could be the desired  $K_{th}$ . To render the same threshold as with sustained load tests, the concentration at the time  $t_R = K_R/K^{\bullet}$  must reach  $C_{eq}(K_R, x_c)$  with a reasonable accuracy as under sustained load. SSRT is performed starting from zero load after fatigue pre-cracking in inert environment. Hydrogenation proceeds affected by the residual stresses caused by pre-cracking. Calculated concentration evolutions are shown in Fig. 4 for simulations of SSRT to determine  $K_{th}$ , supposing  $K_R$  to be the apparent HAC threshold already measured using the sustained load method described in the

previous section. The threshold status corresponding to sustained load case is reached by approaching  $C_{eq}$  in a material point  $x_c$ .

If the critical concentration (1) is stress-controlled, rupture is associated with the maximum tensile stress and occurs at  $x_c = x_{m\sigma}(K_R)$ . To provide sufficient concentration there at the moment of approaching the critical stress intensity factor,  $K_R$  by supposition, the loading must be slow enough to reproduce the result of the sustained load test. A reasonable loading rate may be estimated so that the time  $t_R = K_R/K^\bullet$  to attain this candidate threshold  $K_R$  were close to  $t_{ss}$  for the stationary load situation.

If the critical concentration (1) is strain-controlled, the situation is more complicated. At slow loading rate, concentration evolution in the large-strain zone  $x \lesssim x_{m\epsilon}$  chases after the non-monotonous  $\sigma(t)$ -history which depends on the residual compressive stresses from pre-cracking. Correspondingly, during not too fast loading the concentration in the intensively strained region due to moving peak of stress may temporarily exceed the level attainable there in sustained load test. This was observed in simulations with  $K^\bullet$  up to 0.15 MPam<sup>1/2</sup>/min, but disappeared at 1.5 MPam<sup>1/2</sup>/min, which means that the same fracture criterion (1) may be satisfied at  $x \lesssim x_{m\epsilon}$  earlier than in sustained load case. This is an important point: because of this temporal (and early) concentration peaks, HAC may start at  $K$  below the apparent threshold from the sustained load test, depending on the particular role of stress and strain factors in the critical concentration (1).

### CONCLUSIONS

For sustained load, the adequate testing time to approach the threshold depends on the location of the critical material cell near the crack tip which is associated with the dominating factor of local rupture — strain- or stress-controlled rupture.

Under conditions of dynamic rising loading after fatigue load removal, the crack closure stresses from the pre-HAC loading history may affect hydrogen diffusion towards rupture sites. At slow loading rates, rupture may occur earlier than in the sustained load case at otherwise similar circumstances if critical hydrogen concentration (fracture mechanism) is strain-controlled as the consequence of temporal hydrogen over-saturation peaks which arise owing to the peculiarities of the stress evolution patterns at dynamic loading. Correspondingly, the  $K$ -value for HAC initiation may be lower than the threshold  $K_{th}$  defined from the sustained load test.

*Acknowledgement.* This work was funded by the Spanish CICYT (Grant MAT97-0442) and Xunta de Galicia (Grants XUGA 11801B95 and XUGA 11802B97). One of the authors (VKh) is indebted to Xunta de Galicia and DGICYT (Grants SAB95-0122 and SAB95-0122P) for supporting his stays, respectively, as a visiting scientist and sabbatic professor at the University of La Coruña.

### REFERENCES

- (1) Nelson, H.G., Treatise on Materials Science and Technology. Vol. 25 Academic Press, New York, 1983, pp. 275-359.
- (2) Van Leeuwen, H.-P., Engng. Fract. Mech., Vol. 6, 1974, pp. 141-161.

- (3) Toribio, J. and Kharin, V., Fatigue Fract. Engng. Mater. Struct., Vol. 20, 1997, pp. 729-745.
- (4) MARC User Information, Marc Analysis Research Corp., Palo Alto, 1994.
- (5) Toribio, J. and Kharin, V., Proceedings of ECF12 (in this issue).
- (6) Mayville, R.A., Warren, T.J. and Hilton P.D., J. Test. Eval., Vol. 17, 1989, pp. 203-211.
- (7) Judy, R.W., Jr., King, W.E, Jr., Hauser II, J.A. and Crooker, T.W, ASTM STP 1049, 1990, pp. 410-422.
- (8) Kharin, V. and Toribio, J., Anales Mec. Fract., Vol. 14, 1997, pp. 93-98.
- (9) Turnbull, A., Brit. Corros. J., Vol. 27, 1992, pp. 71-289.

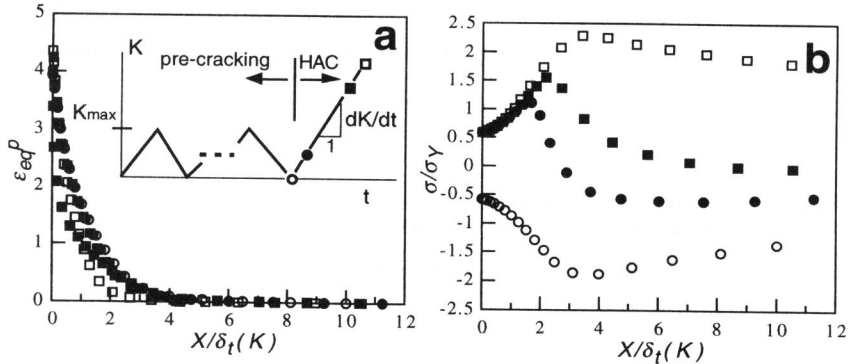


Figure 1. Distributions of  $\epsilon_{ed}^p$  (a) and  $\sigma$  (b) along the crack line at instants of the loading history marked by corresponding symbols in the inserted scheme of the loading path.

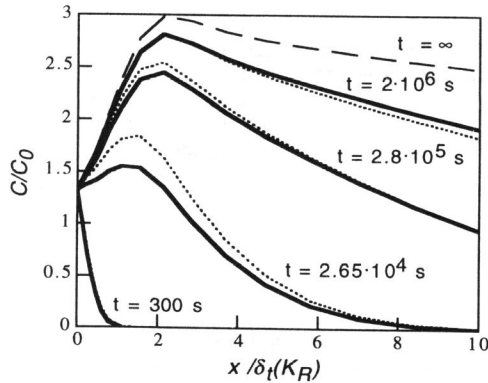


Figure 2. Concentration distributions along the crack line under sustained load conditions at different times  $t$ : finite element solution (solid lines) and asymptotic one (8) (dotted lines). The dashed line shows the  $C_{eq}$ -profile.

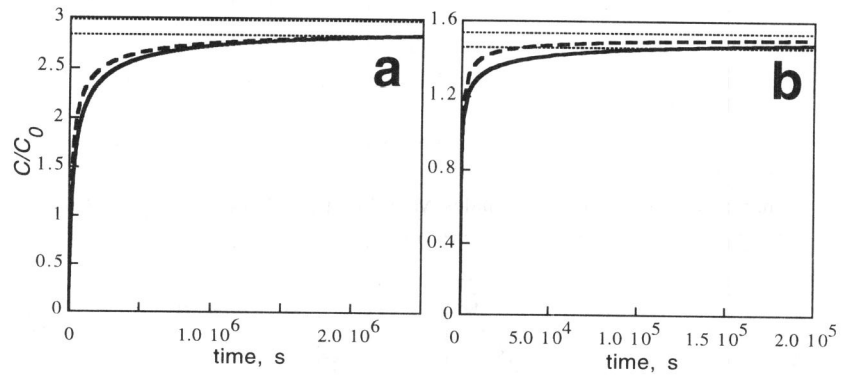


Figure 3. Concentration evolutions according to the finite element solution (solid curves) and asymptotic one (8) (dashed curves) at sustained load: (a) in the points of maximum tensile stress  $x_{m\sigma}$ ; (b) in the high plastic strains region at  $x_{m\epsilon}$ . Horizontal lines mark the 5%-tolerance band near corresponding equilibrium concentration levels  $C_{eq}(x)$ .

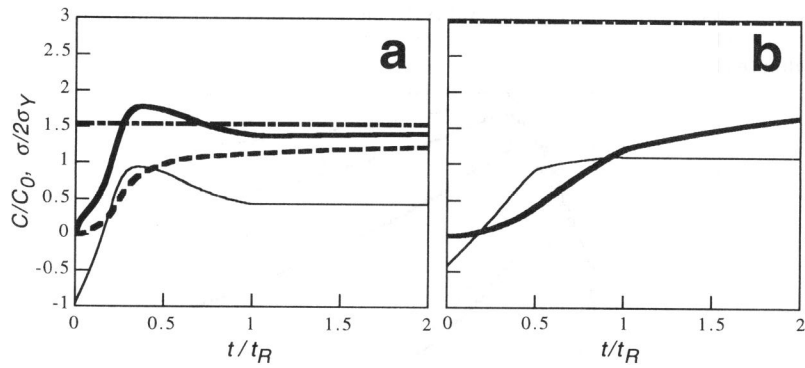


Figure 4. Evolutions of concentration and respective hydrostatic stress patterns at rising load case: (a) at the maximum tensile stress locations  $x_{m\sigma}$ ; (b) at the border of the intensively strained domain  $x_{m\epsilon}$ . Bold lines correspond to  $K^* = 0.15$  (solid) and  $K^* = 1.5 \text{ MPam}^{1/2}/\text{min}$  (dashed) (in (b) these latter concentrations are negligible); thin lines display  $\sigma(t)$ -patterns; horizontal dashed-dotted lines in bold style mark the levels of  $C_{eq}$  in respective locations at  $K = K_R$ .